Efficient design space exploration for spar Floating Offshore Wind Turbines The trilemma of the ultimate, fatigue, and serviceability limit states

Patryniak, Katarzyna; Yeter, Baran; Collu, Maurizio; Coraddu, Andrea

DOI
10.1088/1742-6596/2767/6/062014

Publication date
2024

Document Version
Final published version

Published in
Journal of Physics: Conference Series

Efficient design space exploration for spar Floating Offshore Wind Turbines: the trilemma of the ultimate, fatigue, and serviceability limit states

Journal of Physics: Conference Series **2767** (2024) 062014 doi:10.1088/1742-6596/2767/6/062014

Efficient design space exploration for spar Floating Offshore Wind Turbines: the trilemma of the ultimate, fatigue, and serviceability limit states

Katarzyna Patryniak[a], Baran Yeter[a], Maurizio Collu[a], Andrea Coraddu[b]

E-mail: katarzyna.patryniak@strath.ac.uk
[a] Department of Naval Architecture, Ocean and Marine Engineering, University of Strathclyde, Montrose St, Glasgow, G4 0LZ, UK
[b] Faculty of Mechanical, Maritime and Materials Engineering, Delft University of Technology, Mekelweg, Delft, 2628 CD, Netherlands

Abstract. Floating Offshore Wind Turbines (FOWT) can harness the abundant wind resource in deep-water offshore conditions. However, they face challenges in harsh, unsheltered marine environments. The mean hydro- and aerodynamic loads coupled with fluctuating stochastic wind and wave loads contribute to varied failure mechanisms. Therefore, the serviceability, ultimate, and fatigue limit states are vital in ensuring the safety and reliability of FOWT. This paper investigates how specific loads and states drive the design of a spar-type support structure, utilising a computationally efficient frequency-domain model. This approach combines quasi-static aerodynamic and mooring models with a potential-theory-based radiation-diffraction solver. The serviceability criteria concern the platform and tower top displacements and accelerations. The ultimate and fatigue limit states are assessed for the tower base, the waterline section, and the mooring lines, including the effects of yielding under the bending moment and compressive axial load, column buckling, and tension-tension effects in the mooring lines. The full factorial design of experiments is employed to investigate the non-trivial relationships between the limit states and the various features of the support structure. The results demonstrate that the design of the spar platform above the waterline is mainly driven by fatigue, which results from significant dynamic tilt and increased stress concentration at the platform-tower intersection. On the other hand, the catenary mooring lines' design is mainly driven by the requirements of maximum offset (serviceability limit state) and fatigue.

1. Introduction

Floating Offshore Wind Turbines (FOWT) can harness the abundant wind resources in deep-water offshore conditions, where bottom-fixed structures are not techno-economically feasible. They can access stronger, more consistent, and more uniform wind, thus operating at higher capacity factors [1]. Installed further away from the coast, they minimise interference with other coastal activities and audio-visual, societal, and environmental impacts. However, FOWT are exposed to harsher, unsheltered marine environment conditions. Due to the soft connection to the seabed through a mooring system, the majority of installed FOWT configurations experience larger motions due to environmental loads, with strong interdependence between inertial, wind, wave, and current-driven responses [2].

Notably, the wave-induced rigid body motion response of the platform substantially affects the tower-top motion [3], hence influencing the mean value and variance of the aerodynamic load, leading to fluctuating stresses on system components [4]. Structural loads are further augmented by the loads related to the rigid-body angular displacements and accelerations. Large platform displacements due to aerodynamic loads induce a nonlinear force-displacement relationship of the mooring lines [5], which, together with the wave and turbulent wind loads, leads to significant variability of the mooring tension [6].

The floating offshore system responds not only to large mean aerodynamic loads but also to fluctuating loads due to stochastic wind and wave fields. These distinct sources of load contribute to varied failure mechanisms. In this regard, design limit states play a crucial role in ensuring the safety and reliability of FOWT [7]. They are commonly categorised based on the extremeness and occurrence frequency of the environmental loads into: i) serviceability limit state (SLS), related to the functionality of the structure under normal service loads, ii) ultimate limit state (ULS), related to the load-carrying capacity or ultimate strength of the structural components under the maximum load, iii) fatigue limit state (FLS), related to crack initiation and growth under a sufficient number of stress cycles, and iv) accidental limit state (ALS), related to the structure's resistance to accidental loads and ability to maintain integrity and performance of the structure due to local damage.

Although time-domain nonlinear approaches are generally preferable for the above assessments, they tend to be resource-extensive, and may not be the most suitable design support tools, especially in the initial design stages when the structural design is not yet well defined and a large number of free variables are involved. Therefore, more efficient methods are needed for iterative approaches such as design optimisation. For example, Hegseth et al. [17] performed a FOWT design optimisation with ULS, FLS, and SLS constraints using a frequency-domain (FD) dynamic model.

Complementary to the previous studies, the current work leverages a rapid FD model to systematically investigate the effects of a spar-type FOWT support structure design changes on the system's loads and responses, identifying the design trends and driving factors. This is achieved through i) the development of the models for structural assessment, ii) design space screening as a preliminary step of the design optimisation process, and iii) quantitative assessment of the trade-offs between the three limit states, along with identifying the dominant design factors.

2. Methodology

The study employs design space screening to systematically investigate how quantities of interest (design objectives and constraints) respond to a number of parameters (design variables), which helps better understand the design space behaviour and inform the support structure optimisation process.

The analysis focuses on ULS, FLS, and SLS constraints: maximum platform offset to prevent damage to power export cable or neighbouring facilities (SLS); platform and rotor plane tilt, affecting the aerodynamic efficiency (SLS); nacelle acceleration, affecting the operation of the drivetrain components (SLS); yielding, buckling, and fatigue of the steel sections at the tower base and waterline level (ULS, FLS); mooring line strength utilisation and fatigue damage (ULS, FLS). The accidental limit state is not considered due to the limitations of the frequency-domain model in simulating transient phenomena.

The system considered in this study is the 5 MW NREL reference turbine [9] supported by the OC3 Hywind spar floating supporting structure, with a three-line catenary mooring system [10]. The analyses are performed in an environmental loading scenario similar to DLC 1.2 and 1.3 defined in [11], based on the metocean data obtained for the Scottish sectoral marine plan "NE8", which is an offshore site planned for floating offshore wind farm deployment. For the

FLS assessment, the mean wind speeds from cut-in to cut-out speed ($3-25$ m/s) are binned into 2 m/s bins, and the expected values of the significant wave height and peak period, conditioned on the wind speed (and wave height), are defined for each bin. The ULS assessment is done for the condition of rated wind speed (11.4 m/s), i.e., the condition of maximum aerodynamic thrust load.

2.1. Frequency-domain model of dynamics

The FD dynamic model is based on the Multidisciplinary Design Analysis methodology previously presented by the authors [8], with different disciplines solved by specialised routines coupled in a numerical framework. The FD approach offers the efficiency needed for fatigue analysis, as the alternative time-domain approach can be prohibitively expensive when performing multiple simulations for the full range of environmental conditions and random realisations [6]. While TD solutions can typically take time in the order of hours, FD approaches can provide solutions in minutes for similar problems. Given an environmental condition, an iterative procedure yields the mean offset of the platform, considering the hydrostatic, mean mooring, and mean aerodynamic loads. Mooring loads are computed by a quasi-static solver, while aerodynamic loads are computed by a Blade Element-Momentum solver. Fluctuating hydrodynamic loads from stochastic waves are obtained for this converged equilibrium position based on the solutions of the FD equations of motion with the wave excitation. The hydrodynamic loads are computed using a Boundary Element Method solver.

The model has been verified against the results obtained with OpenFAST, set up to resemble the capabilities of the current model (i.e., without considering the flexible modes, second-order hydrodynamics, and turbulent wind), for the original design of OC3 spar with 5MW reference rotor [9, 10]. As presented in Table 1 for the case of rated wind speed conditions, the motion response, tower base bending moment, and mean mooring tension predictions reasonably match the higher-fidelity model's results. However, there is a significant discrepancy in the mooring line tension standard deviation. Although the quasi-static mooring model employed in the current work cannot accurately predict the tension range, it can capture the design trends well for most of the design space, as shown in Figure 1.

Table 1: Model verification in rated wind

Response	OpenFAST	Current	OpenFAST	Current
	Mean		Standard deviation	
Surge (m)	24.84	25.28	0.12	0.11
Heave (m)	-0.53	-0.61	0.02	0.02
Pitch (deg)	4.97	4.90	0.07	0.06
Hub ac. (m/s^2)	-	-	0.17	0.15
$M_{y,twr}(kNm)$	86156.3	99169.6	6257.3	4967.7
$T_{moor,2}$ (kN)	1238.2	1250.9	8.4	1.2

Figure 1: Mooring line tension st. dev. against design variables.

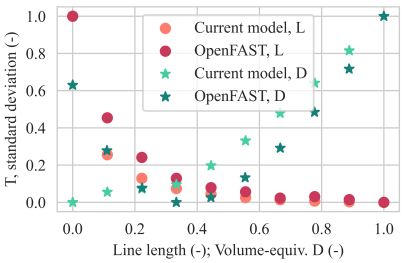

2.2. Loads model

The ULS and FLS loads were assessed for three locations of interest: the tower base (i.e., the top of the transition piece), a section of the floater at the waterline, and the mooring line link at the fairlead.

2.2.1. Ultimate limit state loads model The characteristic mooring line tension for the most heavily loaded line required for the ULS check was formulated as a sum of the characteristic mean line tension T_{C-mean} (due to pretension and mean wind load) and the characteristic dynamic

line tension T_{C-dyn} (due to fluctuating wave load). The dynamic component was assessed by measuring the variation in tension between two specific positions of the platform: one at the mean position and the other at one standard deviation above the mean position.

The characteristic strength of the chain is obtained from the minimum breaking strength S_{mbs} of a single link as:

$$S_c = 0.95 S_{mbs} \tag{1}$$

Partial safety factors are applied to the mean and dynamic characteristic tension so that the utilisation factor (and ULS design criterion) can be finally formulated as:

$$\frac{T_{C-mean}\gamma_{mean} - T_{C-dyn}\gamma_{dyn}}{S_c} \leq 1 \tag{2}$$

In this study, the quasi-static mooring model necessitates higher partial safety factors. Consequently, both γ_{mean} and γ_{dyn} are set at 1.70.

For the tower and floating platform sections, two ULS failure criteria were assessed: i) yielding under bending moment and compressive axial load, ii) column buckling, as recommended in [12]. The von Mises yield criterion was formulated based on the ratio between the material's yield stress (σ_{yield}) and the maximum von Mises stress on the structure (σ_{max}) as follows:

$$\frac{\sigma_{max}\gamma_r\gamma_m}{\sigma_{yield}} \leq 1 \tag{3}$$

γ_m and γ_r are the partial safety factors for material and resistance, applied to accommodate uncertainties related to load and resistance calculations, as well as material properties, as outlined in reference [13]. They are assigned values of 1.1 and 1.25, respectively. The buckling criterion was formulated based on the characteristic buckling load ($\sigma_{j,Sd}$), the shell buckling strength (f_{ksd}), and the material factor γ_m:

$$\frac{\sigma_{j,Sd}}{f_{ks}/\gamma_m} \leq 1 \tag{4}$$

The characteristic buckling load was calculated, including the effects of the design axial load due to the weight of the tower and the RNA, as well as the design bending load due to the moments of the aerodynamic thrust, aerodynamic drag on the tower, and inclination and acceleration of the tower and RNA. The effects of the circumferential stress due to external pressure and shear stress due to torsional moments and shear force were neglected.

2.2.2. Fatigue limit state loads model Mooring lines fatigue capacity calculation follows the DNV suggested S-N approach [14]. For each environmental state i, the standard deviation of the wave-frequency tension is calculated as the difference between the tension in two positions: i) mean plus standard deviation of surge displacement (x_{max}), and ii) mean surge offset (x_{mean}):

$$\sigma_{T,i} = T_i|_{x_{max,i}} - T_i|_{x_{mean,i}} \tag{5}$$

The nominal stress range (double amplitude) is then given as the tension range divided by the nominal cross-section area of the chain:

$$\sigma_{S,i} = \sigma_{T,i}/(2\pi d^2/4) \tag{6}$$

The fatigue damage can be computed as:

$$d_i = \frac{n_i}{a_D} E[\sigma_{S,i}^m] \tag{7}$$

Since the current approach neglects the low-frequency loads, the stress process can be assumed narrow-banded (Rayleigh distributed). Therefore, the expected value of the nominal stress ranges raised to the power m is given by:

$$E[\sigma_{S,i}^m] = (2\sqrt{2}\sigma_{S,i})^m \Gamma(\frac{m}{2} + 1) \tag{8}$$

The number of stress cycles (n_i) for the $i-th$ environmental state is computed as the ratio of the product of the probability that state p_i and the design life with the wave peak period T_p:

$$n_i = p_i T_D / T_p \tag{9}$$

The FLS criterion is then formulated as:

$$\sum_i d_i \leq 1 \tag{10}$$

This analysis solely focuses on tension-tension fatigue, excluding the out-of-plane bending effects Furthermore, 50% of the chain's corrosion allowance is taken into account.

The calculation of the fatigue damage for the steel structures follows a similar procedure. The nominal stress at a section of interest is calculated based on the fluctuating bending moments due to the system's pitching behaviour in waves (pitch displacements and acceleration). Then, the hotspot stress range is calculated as the product of the nominal stress at a given section and the appropriate stress concentration factor (SCF). These factors are applied to account for geometric discontinuity (e.g., slope between two sections of varying diameters), complexity of connections, and manufacturing tolerances in accordance with [15]. On the resistance side, the $S-N$ curves for steel tubular structures in seawater without cathodic protection are used. Due to the current constraints of the dynamic model, which is still under development, the fatigue damage caused by the low-frequency, wind-driven load is not accounted for in this analysis.

2.3. Design of experiment

The design space screening involves the main dimensions of the floating support structure (waterline level radius, tower base radius, and wall thickness), as well as some of the main parameters that define the design of the catenary mooring system: unstretched mooring line length and its volume-equivalent diameter, as illustrated in Figure 4. Even though exploration of the total space of five variables would be ideal, the two sets of variables are considered separately. That is, the effects of varying steel structure design on the mooring system performance, and vice versa, are not analysed here. The remaining design features are kept fixed at the OC3 Hywind spar reference values, which reduces the size of the design matrix.

The full factorial sampling method is applied to identify the design trends. Although more computationally expensive than alternative sampling methods (e.g., Latin Hypercube), the full factorial design provides a regular grid to clearly illustrate the gradual changes in the responses across the domain.

A total of 612 designs were analysed with 12 simulations per design (1 in ULS and 11 in FLS conditions). The hydrodynamic solver ran in parallel using 32 logical processors at 2.1 GHz, and the rest of the model ran in serial mode. The entire study took about 6 hours in total, which is a significant gain over the state-of-the-art time domain approaches [16] (although there is still scope for improvement with better utilisation of multiprocessing across the whole model).

3. Results and Discussion

The results of the study described above are presented for the mooring lines design variables first, followed by the study of the sensitivity of the limit states to the tower and floating substructure features. The FLS, ULS, and buckling criteria presented in the plots were capped at 1, which marks the feasibility boundary.

3.1. Sensitivity to mooring line variables

Figures 2-3 present the serviceability criteria (maximum offset and tilt) as a function of the mooring line length and volume-equivalent line diameter.

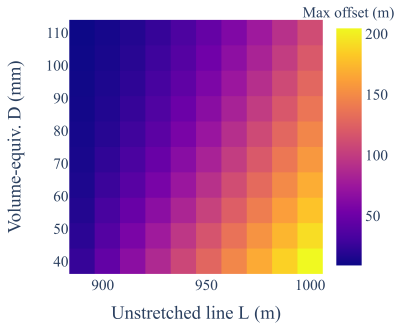

Figure 2: Maximum offset in the rated conditions.

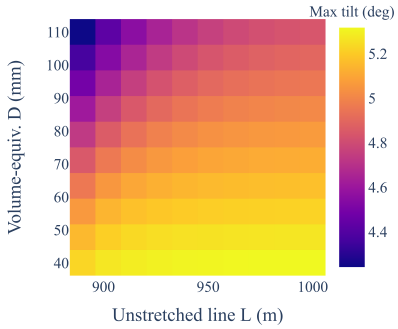

Figure 3: Maximum tilt in the rated conditions.

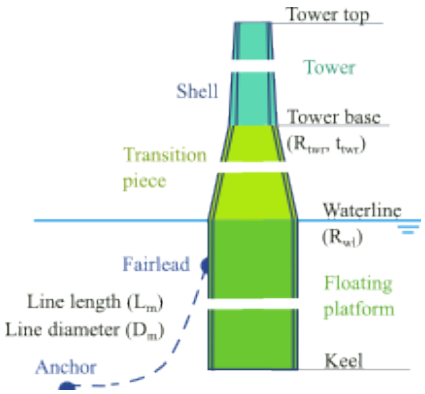

Figure 4: Design variables.

As expected, longer mooring lines of lower diameter result in a softer system with larger offset and tilt. Assuming deep water conditions (water depth of 320 m), about half of the designs considered exceed the offset of 40% of the water depth. The impact of the mooring design on tilt is less pronounced, as expected for the particular spar-type platform considered in this study. As such, tilt seems not to be a factor that would drive the moorings' design.

Figures 5-6 present mooring line strength utilisation and fatigue damage as a function of mooring line length and volume-equivalent line diameter.

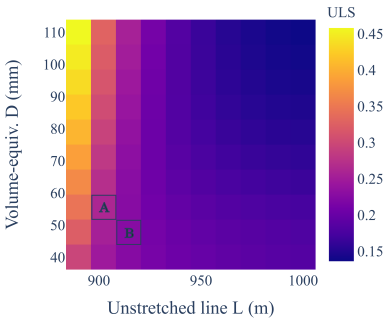

Figure 5: Mooring line strength utilisation.

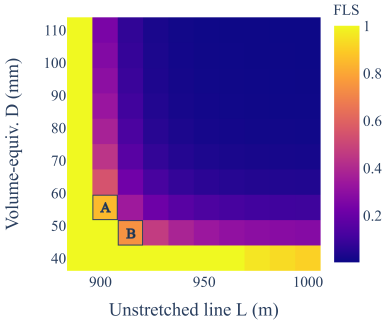

Figure 6: Mooring line fatigue damage.

As the line length decreases, the mooring system becomes stiffer, resulting in higher mean and dynamic tension, which leads to increased strength utilisation and fatigue damage. Lines below about 900 m in length or below 50 mm volume-equivalent diameter result in unfeasible designs through exceeding the FLS limit (note that these values are indicative only, as the exact limits highly depend on the mooring tension range solution, which might be inaccurate coming from a quasi-static mooring model). Increasing the chain diameter helps to offset the negative effect of short lines to an extent. Even though a heavier chain results in higher pretension, which generally negatively affects ULS compliance, it significantly increases the chain link's resistance to fatigue by increasing the nominal cross-section area of the chain.

Both the ULS and FLS criteria are more sensitive to the line length change in the short-line-length range. Varying the line length within a small range between 900 – 920 m (about 20% of the range) almost entirely accounts for the variation in limit states.

All in all, the FLS criterion was the only active constraint, eliminating 17% of the designs considered. Within the feasible subspace, two solutions stand out as good candidate designs of likely lowest cost:

- Design 1: Line length of 914 m and diameter of 55 mm,
- Design 2: Line length of 926 m and diameter of 48 mm.

The choice between the two designs would depend on the sensitivity of the cost to the line length and diameter, which is not readily available, as it depends on the current market prices and availability, among other factors. Note that this is a rough indication due to the coarseness of the results; constraints not considered in this analysis may also affect the assessment.

3.2. Sensitivity to tower and floating substructure variables

Figures 7-12 present the mean and dynamic pitch displacements, maximum offset, tower top acceleration, waterline section yielding and fatigue damage criteria as a function of the waterline section and tower base outer radii.

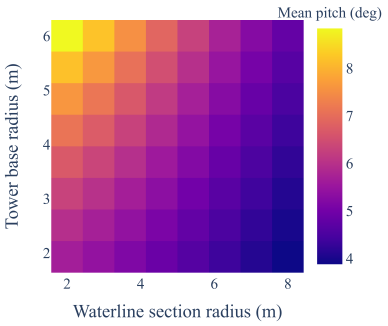

Figure 7: Mean pitch displacement.

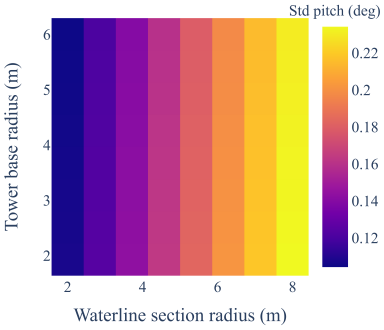

Figure 8: Dynamic pitch displacement.

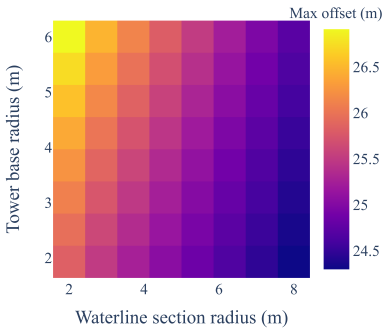

Figure 9: Maximum offset.

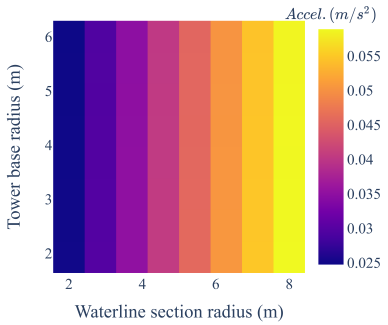

Figure 10: Tower top resultant acceleration in rated conditions.

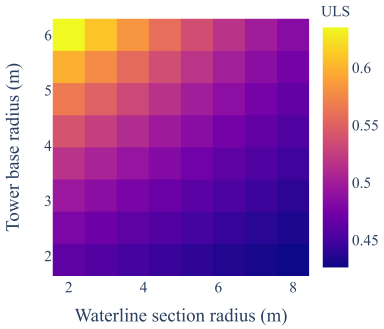

Figure 11: Waterline section strength utilisation.

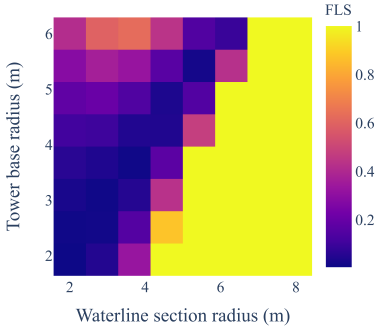

Figure 12: Waterline section fatigue damage.

The results show that the structure is more susceptible to the reduction of operational efficiency and failure due to excessive motions leading to fatigue rather than the ultimate load-carrying capacity issues. As shown in Figures 8 and 10, the dynamic part of the pitch motion and tower top acceleration increase with the water line radius as the platform becomes less transparent to

waves. A larger tower base radius partly mitigates this effect by increasing the system's inertia. These increased motions also result in higher fatigue damage, which cannot be sufficiently offset by an increased sectional area. The combination of a large waterline and small tower radii exacerbate fatigue due to increased wave-induced motion and transition piece angle, leading to high stress concentration factors.

For the original tower design with a base radius of 3.25 m, the waterline radius must be below 5 m to avoid excessive wave-drive motion and stress concentration, which would lead to excessive fatigue accumulation in the waterline section. In fact, the designs where the tower base and waterline section radii are equal show the least fatigue, which can be observed in 12 as a dark blue "crest" along the design space. In these cases, the transition between the floating substructure and the tower is smoothest, resulting in minimum stress concentration at the sections concerned. Interestingly, even though the maximum offset, tilt, and tower top acceleration are within acceptable ranges, they indirectly drive the support structure's design through their effect on fatigue.

The ULS criterion tends to decrease with the waterline radius increasing, as the mean load dominates over its fluctuation component: higher waterplane area and moment provide better stability and lower stresses, resulting in lower ULS. A higher tower base radius shifts the total centre of gravity upward, decreasing the gravitational stiffness of the system and acting against the positive trend of increasing waterline radius. However, within the range of parameters considered, the ULS criterion is never violated and, therefore, is not a design-driving factor, as far as the waterline section is concerned.

Figures 13-14 present the tower base section yielding and fatigue damage criteria as a function of the waterline section and tower base outer radii.

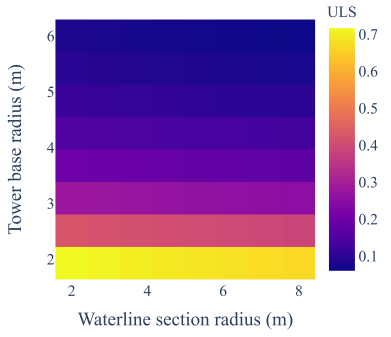

Figure 13: Tower base section strength utilisation.

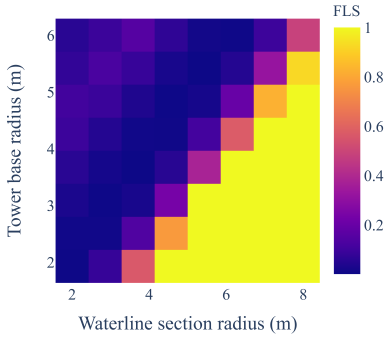

Figure 14: Tower base fatigue damage.

The tower base yielding criterion (ULS) appears to be dominated by the effect of the tower base diameter and is relatively unaffected by the waterline section radius. A higher tower base radius gives a larger cross-section area, lowering the stress experienced at the section. Again, all configurations pass the tower base ULS check.

Regarding the fatigue damage, trends similar to these observed for the waterline section are seen. There seems to be a clear division of the design space into feasible and unfeasible regions. The feasible region is mostly made out of configurations where the tower base is about the size of the waterline section or larger. Since the tower diameter should, in principle, be smaller or equal to the waterline section diameter, the feasible space further reduces to a small subset where the two sections have very similar dimensions.

So far, the wall thickness of the tower has been kept at its original value of 0.027 m. As illustrated in Figures 15-16, derived for the case of the original waterline section radius, increasing

the tower wall thickness generally reduces the yielding. A more complex, non-monotonic trend is observed regarding the FLS criterion with a minimum around the middle of the range of wall thickness considered. This is linked to the impact of the stress concentration factor, which is not only a function of the outer radii but also the wall thickness, as can be seen in Figure 17.

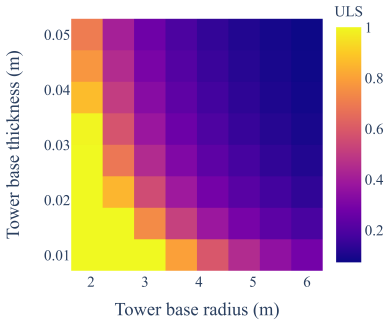

Figure 15: Tower base section strength utilisation – the effect of wall thickness.

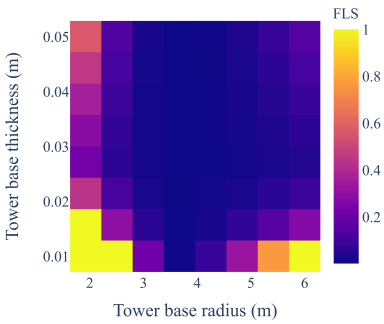

Figure 16: Tower base fatigue damage – the effect of wall thickness.

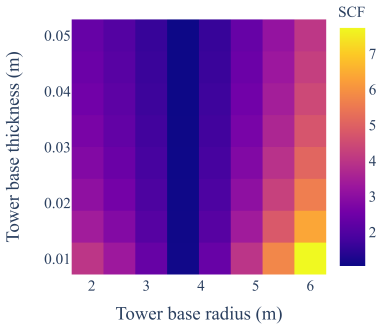

Figure 17: Stress concentration factor for conical transition at the tower base.

Lastly, buckling of the tower seems not to be an issue for any configurations considered as long as the wall thickness remains at or above the original value, as confirmed by Figures 18-19. As expected, it presents trends very similar to these observed for the yielding criterion at the tower base. Based on the results, the tower is likely to reach the buckling criterion limit before any yielding occurs.

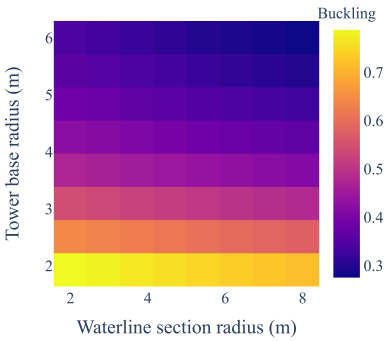

Figure 18: Tower buckling.

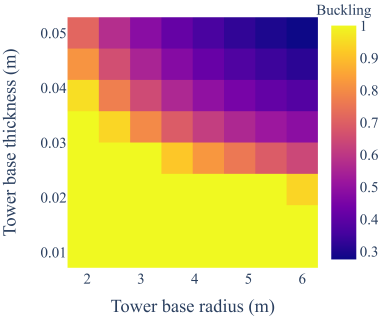

Figure 19: Tower buckling – the effect of wall thickness.

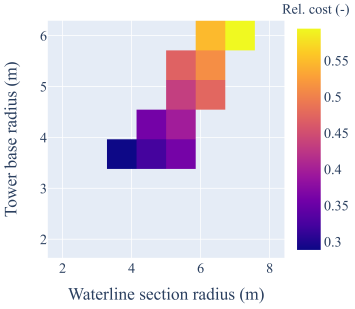

Figure 20: Material cost normalised to $0-1$. Only feasible designs are shown.

Considering all limiting criteria, the design of the tower and floating substructure above the waterline level is mostly driven by fatigue and buckling, except for the very small tower wall thickness cases where yielding becomes an issue. This agrees well with previously published results, for example [17]. Satisfying the FLS criterion requires that the radii of the waterline and tower base sections remain comparable and that the tower wall thickness is larger than about 0.02 m (for the system and conditions considered in this study). Additionally, the ULS constraint imposes the requirement for the tower base diameter to be larger than about 2.0 m, which, for some small wall thickness values, is further increased by the buckling constraint. That said, for the case of the original wall thickness of 0.027 m, the most economical feasible design would be that of the waterline section diameter of 3.71 m and tower base radius of 3.67 m, as demonstrated in Figure 20. Note that the specific design recommendations are highly

dependent on the accuracy of the dynamic model. Although the ULS and FLS loads computation already includes DNV-recommended safety factors, additional modelling uncertainty analysis is recommended. Likewise, this above analysis concerned a simplified (unstiffened) structure, as appropriate in the early pre-FEED stages (conceptual design and feasibility studies).

4. Conclusion

The paper presented an efficient frequency-domain method for early design stage limit states assessment, including the ultimate, fatigue, and serviceability limit states for three critical structural components of a floating wind turbine: the tower base and waterline sections, as well as the mooring chain at the fairlead. The sensitivity of the three limit states to the structural dimensions of the floating support structure was studied based on a full factorial design of experiments. The results allowed for the identification of the feasible and unfeasible design regions and provided insight into the design trends within the feasible subspace. Although the observations are highly case-specific, the most important trends identified include:

- Mooring lines' design had a vast impact on the maximum offset of the platform, affecting the serviceability limit state, as expected.
- Mooring lines' design was mainly driven by the fatigue consideration and not by the strength utilisation.
- The serviceability criteria (maximum offset, tilt, and tower top acceleration) were not exceeded for any floating substructure configuration. However, they contributed to increased fatigue loads in the steel sections, indirectly driving the design.
- The tower was likely to experience buckling before any yielding began. Likewise, failure through the fatigue mechanism was more likely than that due to maximum load (ULS).

Note that the above conclusions are only valid for the particular spar-type FOWT studied and might also depend on the accuracy of the dynamic model used in the study. The model has been verified within the scope presented in this paper, however, the generalisation of the conclusions requires further study. Although multiple simplifications were made, including the use of a linearised model of dynamics and (for the time being) neglecting the impact of the turbulent wind load, this rapid method allows for an initial design space screening to limit the feasible configurations, which can contribute to increasing the efficiency of the later design and analysis processes. If the traditional iterative design approach is followed, this method allows the selection of a limited set of candidate designs which might then be analysed by more expensive, higher-accuracy tools. Alternatively, modern optimisation approaches can benefit from the methodology presented in this paper through informed reduction of the design variables ranges (bounds) as a preprocessing step before the actual optimisation process.

4.1. Acknowledgments

This work was supported by the University of Strathclyde REA 2022. The authors would like to acknowledge the support of the John Blackburn Main Scholarship and the IMarEST.

5. References

[1] Smith A Z 2023 UK offshore wind capacity factors. Retrieved from https://energynumbers.info/uk-offshore-wind-capacity-factors on 2023-08-12.
[2] Bachynski E E and Moan T 2012 Design considerations for tension leg platform wind turbines *Marine Structures* **29**
[3] Huang Y and Wan D 2020 Investigation of Interference Effects between Wind Turbine and Spar-Type Floating Platform under Combined Wind-Wave Excitation *Sustainability* **12** 246
[4] Veldman P N 2020 Essentials in Coupled Dynamics of Floating Offshore Wind Turbines: A research on simplified modelling of a Floating Offshore Wind Turbine *Master thesis*
[5] Liu Y and Xiao Q and Incecik A and Peyrard C and Wan D 2017 Establishing a fully coupled CFD analysis tool for floating offshore wind turbines *Renewable Energy* **112** 280-301

[6] Ma KT, Luo Y, Kwan T and Wu Y 2019 Mooring System Engineering for Offshore Structures *Elsevier Cambridge, MA: Gulf Professional Publishing* **12**
[7] IEC 61400-1:2019 Wind energy generation systems. Design requirements.
[8] Patryniak K, Collu M and Coraddu A 2022 Multidisciplinary design analysis and optimisation frameworks for floating offshore wind turbines: State of the art *Ocean Engineering* **251**
[9] Jonkman, J. 2010 Definition of the Floating System for Phase IV of OC3. *National Renewable Energy Laboratory (NREL)*
[10] Jonkman, J. and Butterfield, S. and Musial, W. and Scott, G. 2009 Definition of a 5-MW Reference Wind Turbine for Offshore System Development. *National Renewable Energy Laboratory (NREL)*
[11] The British Standards Institution 2019 EN IEC 61400-3-1:2019 Wind energy generation systems. Design requirements for fixed offshore wind turbines
[12] DNV 2013 DNV-RP-C202. Buckling Strength of Shells.
[13] DNVGL 2018 DNVGL-ST-0126 Support structures for wind turbines.
[14] DNV 2013 Offshore Standard DNV-OS-E301. Position Mooring.
[15] DNV 2014 DNV-RP-C203 Fatigue design of offshore steel structures.
[16] National Renewable Energy Laboratory 2023 OpenFAST documentation. Performance. Retrieved from https://openfast.readthedocs.io/en/main/source/dev/performance.html
[17] Hegseth, J M and Bachynski, E E and Martins, J R R A 2020 Integrated design optimization of spar floating wind turbines *Marine Structures* **72**